Princeton Plasma Physics Laboratory

PPPL- 4798

PPPL- 4798

Disruption Analysis and Response Implicattions of Passive Plates for the NSTX Upgrade

Yuhu Zhai, Peter Titus, Art Brooks, and Ron Hatcher

August, 2012

PPPL PRINCETON PLASMA PHYSICS LABORATORY

Prepared for the U.S. Department of Energy under Contract DE-AC02-09CH11466.

Princeton Plasma Physics Laboratory
Report Disclaimers

Full Legal Disclaimer

Trademark Disclaimer

PPPL Report Availability

Princeton Plasma Physics Laboratory:

http://www.pppl.gov/techreports.cfm

Office of Scientific and Technical Information (OSTI):

http://www.osti.gov/bridge

Related Links:

U.S. Department of Energy

Office of Scientific and Technical Information

Fusion Links

Disruption Analysis and Response Implications of Passive Plates for the NSTX Upgrade*

Yuhu Zhai, Peter Titus, Art Brooks, Ron Hatcher

Princeton Plasma Physics Laboratory, Princeton, NJ, USA

The NSTX upgrade project requires analysis qualifications of existing vacuum vessel and passive stabilizing plates for increased plasma performance. Vertical stability is critically dependent on the passive conducting structure that surrounds the plasma. In this paper, the passive conducting structure is analyzed for the upgrade condition during plasma disruption to ensure the level of stress in the stabilizing plates and the fastener is within its design limits. The counter-bore of the passive plates for bolting is evaluated in details and counter-bore bushing is redesigned to prevent shear failure during disruptions as a result of high pulling and pushing forces, particularly for support at the corner bolts.

I. INTRODUCTION

The National Spherical Torus eXperiment (NSTX) is a large-scale spherical tokamak magnetic fusion facility currently under upgrade construction at Princeton Plasma Physics Laboratory. The NSTX upgrade will double the toroidal field, plasma current, NBI heating power and increase pulse length from 1-1.5 s to 5 s for accessing reduced collisionality [1-2]. The upgrade performance increase requires engineering qualifications of all remaining components such as the vessel and the passive plate structures for higher disruption loads. Plasma vertical stabilization is provided by eddy currents flowing in the passive plates which resist plasma motion along with feedback control of the PF coils. To this end, the passive structural components are analyzed in details with accurate 3D electromagnetic and mechanical analysis under various disruption scenarios described in the general requirements document (GRD) [2]. The worst disruption loads on the primary plates are from P1 to P5 VDEs during 10 ms translation followed by a 1 ms fast quench. Previous analysis based on a vector potential transfer approach using 2D electromagnetic simulations indicates significantly higher disruption loads under upgrade performance [3].

Since disruption loads on the center stack, the vessel and its components are used as input for a number of other global and local analyses for the NSTX upgrade, it is important to validate the methodology used in previous passive plate disruption analysis and cross check the magnetic field distribution and eddy current flowing on the passive plates during plasma disruption. In this paper, the passive plates are modeled in Opera 3d, together with the vessel, the support bracket and connecting bolts for electromagnetic analysis and resultant structural response during plasma disruptions. In particular, skin effect, which is significant in the copper plate during disruptions and fast VDEs, is captured more effectively from the Opera 3d analysis. With a ~2-3 mm skin depth of the passive plate during a millisecond disruption, eddy current flowing on the plate penetrates only ~1/5 into the plate thickness. While the global vector potential transfer approach [3] is more advantageous for efficient static and dynamic analysis of complex structures, the Opera 3d-based global EM simulation provides a consistent way of capturing component resistivity as well as skin effect in highly conductive structures such as the passive plate. It also corrects a fundamental error in the expectation that the vector potential solution from a 2D simulation with an effective toroidal passive plate resistivity could be transferred to a more detailed 3D electromagnetic model. In addition, a new Opera to ANSYS disruption load mapping procedure has been established for an integrated mechanical analysis. The results are compared with that of a full 3D EM and mechanical coupled analysis using classic ANSYS. The net toroidal current flowing in the plate is ~200 kA from the worst case during P1 to P5 VDE and fast disruption. The resultant peak force of one primary plate pushing against its support bracket is ~60 kN at the end of the plasma translation and the resultant peak force pulling the plate is ~75 kN at the end of the 1 ms fast disruption following the plasma translation.

Although results indicate that the half inch plates meet design limit for the upgrade performance, counter-bore of the primary and secondary plates for bolting is evaluated in details, and the counter-bore bushing is redesigned to prevent shear failure during disruptions as a result of high pulling and pushing forces, particularly for support at the corner bolts.

II. Model Description

Since the NSTX vacuum vessel, the passive plates and supporting brackets are complicated non-axisymmetric 3D structures, the eddy current flowing pattern is difficult to predict in a simplified 2D electromagnetic analysis using averaged electrical conductivity measured in all passive structures. A 3D Opera electromagnetic model is generated for accurate disruption analysis and a new Opera to ANSYS load mapping procedure has been established for extracting the resultant stresses. The new model includes not only the primary and secondary

passive plates, but also the supporting brackets with connecting bolts, the vacuum vessel and the center stack casing. The model in Figure 1 shows the NSTX coils and a 60 degree section of the passive structure components.

The background fields from the 3D Opera model are benchmarked against 3D Maxwell results as well as analytical solutions [4-5]. The field from circular shape plasma during disruption has also been checked against previous 2D results using the same averaged electrical conductivities for the passive plates as shown in Table 2. However, the 2D analysis assumed an axisymmetric condition with a uniform conductivity based on measured disruption current flows in the vessel/passive plate system. This assumption gives ~18 mm skin depth of the lower primary plate for the 1 ms disruption (larger than the plate thickness) and the skin depth increases to 57 mm for 10 ms VDEs. This could greatly overestimate the induced eddy current flowing in passive plates since the actual skin depth shown in Table 1 is only 1/5 of the plate thickness.

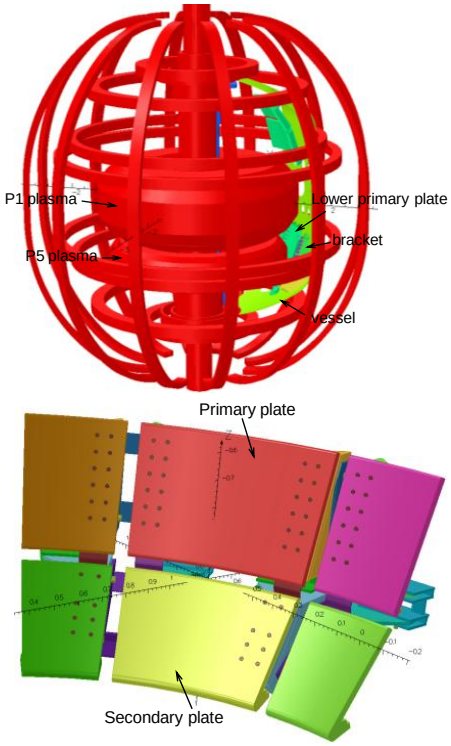

Figure 1 NSTX PF, OH and TF coils with 60 degree model of passive plates and support bracket, VV, and CS casing (top); passive plates with support brackets and the connecting bolts (bottom).

III. Passive Plates

The NSTX passive conducting plates consist of four toroidal rings of 48 independent copper plates covered by graphite tiles. The plates are electrically connected to each other indirectly through the high resistive mounting bracket welded on the vacuum vessel. The plates are mainly used for the control of plasma vertical stabilities. The electrical conductivity and skin depth during 1 ms disruption is listed in Table 1 below. Table 2 listed the effective conductivities for NSTX materials from DC measurements directly used in previous 2D analysis.

Table 1 Electrical conductivity and skin depth of NSTX materials for 1 ms disruption

	Conductivity (S/m)	Skin depth (mm)
Plate (85% Cu)	5.07×10^{7}	2.25
Bracket (SS)	1.389×10^{6}	13.5
Vessel (SS)	1.389×10^{6}	13.5
Casing (Inconel)	7.576×10^{5}	18.3

Table 2 Effective conductivities for NSTX materials from DC measurements directly used in previous 2D analysis

	Conductivity (S/m)	Skin depth (mm)
Upper primary plate	8.387×10^{5}	17.4
Upper secondary plate	6.113×10^{5}	20.4
Lower primary plate	8.207×10^{5}	17.6
Lower secondary plate	6.668×10^{5}	19.5
Vessel (SS)	1.389×10^{6}	13.5
CS casing (Inconel)	7.576×10^{5}	18.3

IV. Model Validation

Figure 2 presents the plasma disruption scenarios defined in the GRD for NSTX upgrade [2]. Figure 3 presents comparison of the radial magnetic field between results from previous 2D axisymmetric model and that from the 3D 60 degree model from circular plasma at 10 ms during P1-P5 slow VDEs.

For model validation, the same conductivities listed in Table 2 from NSTX DC measurement data are used in the 3D Opera model. The field contour lines in Figure 3 from 2D model agree well with color contours shown in the left panel of Figure 4 from the 3D model. In Figure 3, the radial field penetrates through the lower secondary plate from ~0.9 T in the middle of the front surface to ~0.6-0.7 T at the plate back surface. This is because averaged electrical conductivities in Table 2 are used for the passive plate; therefore skin depth is much larger than that of copper conductivity during disruption. The field during disruption penetrates through the plate thickness. The vertical field plots show a similar agreement between the 2D and 3D axisymmetric models using the measured material conductivities.

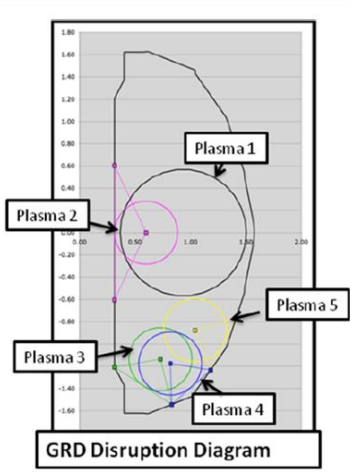

Figure 2 Plasma disruption scenarios described in GRD; we focus on mid-plane disruption and P1-P5 slow and fast VDEs. P5 is located in between the primary and secondary plates.

Figure 4 presents the radial fields from 3D models using NSTX measured effective conductivity (left) and copper conductivity (right) for the plate with circular shape plasma at 10 ms during P1-P5 slow VDEs. Very different from figure 3 and the left plot, field on the right penetrates into only a fraction of the plate thickness during disruption due to significant skin effect. Part of the plate in the back is shielded by eddy current flowing in the front surface. Therefore, the net eddy current load is much smaller than that from the model using the measured plate and bracket averaged conductivity during disruption.

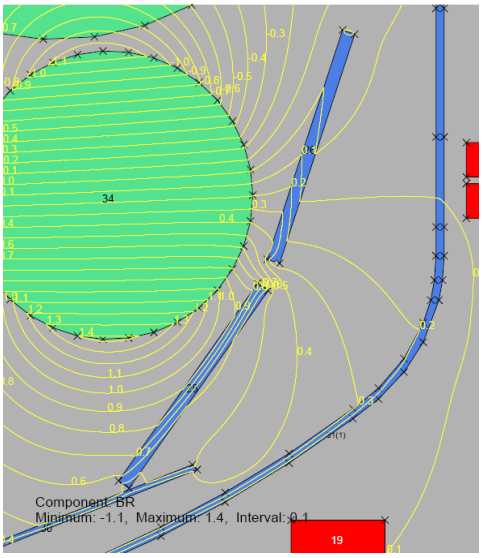

Figure 3 Radial field (in Tesla) from 2D axisymmetric model during P1-P5 slow VDE at 10 ms; close agreement with 3D model if same conductivity is used

V. Matched Electrical Conductivity

In the 3D Opera model, the passive plates are electrically connected with the support bracket only through the long bolts. The steel shim plate underneath the passive plate is not included. The electrical conductivity of the SS bolts and the support bracket is adjusted for the NSTX passive structure composite to match the measured conductivity for the eddy current loop consisting of the passive plates, support bracket, connecting bolts and the vacuum vessel.

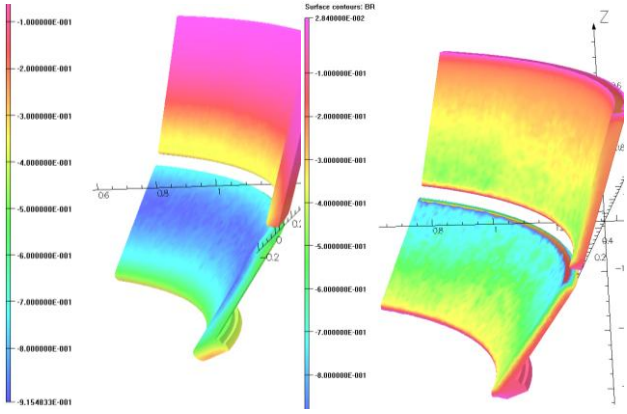

Figure 4 Radial fields during P1-P5 slow VDE at 10 ms from 3D models using NSTX measured effective conductivity (left) and the CrCuZr conductivity (right); skin depth effect is clearly seen through plate thickness if CrCuZr conductivity is used.

To match the measured overall passive structure electrical conductivity, the current flow solver in Vector Fields is used and two 60 degree sector models are created. In the first model, the measured conductivity is used and the net conductance for the 60 degree sector is obtained by applying zero voltage on one side and 1 volt at the other side of the sector to force current flow into the plate. In the second model, plates, bolts and bracket are included to form the conducting path from plate to bolt and bracket so part of eddy current flows into the vessel. The same voltage conditions are applied to obtain the net conductance for the 60 degree sector. The resistance or conductance is matched for the two models by adjusting iteratively conductivity in the bolt and the bracket. The matched conductivities are listed in Table 3.

Table 3 Electrical conductivities matched with NSTX measurement and used for 3D analysis

	Matched conductivity (S/m)
Passive Plate	5.07×10^7
LPP Bracket/bolt	5.2×10^6
LSP Bracket/bolt	1.0×10^6

VI. Disruption Loads

The disruption force and moment on the passive plates are extracted from the Opera 3d results for mechanical stress analysis. Figure 5 presents the net disruption forces and moments on the primary and secondary plates during P1 to P5 slow VDE and followed by 1 ms fast disruption. The resultant peak force of one primary plate pushing against its support bracket is ~60 kN at the end of the plasma translation; the resultant peak force pulling the plate is ~75 kN at the end of the fast plasma disruption.

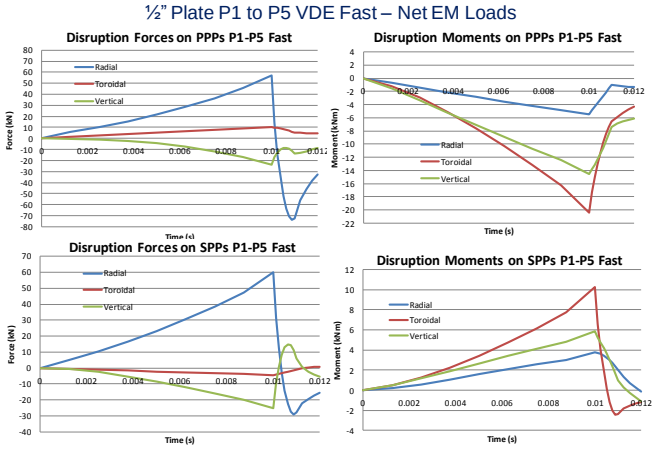

Figure 5 Disruption force and moment on primary (upper) and secondary (lower) passive plates during P1-P5 slow VDE and fast disruption.

VII. Static Structural Analysis

The elemental disruption force density extracted from the Opera 3d results is mapped onto an ANSYS Workbench model. The new structural model includes the plate, bolts and the support bracket. The liquid lithium divertor (LLD) and VV are not included in the mechanical analysis. Figure 6 shows the comparison of eddy current density flowing in the lower passive plates using Opera versus that using classic ANSYS. The max linearized membrane stress on the primary plate is ~200 MPa as indicated in Figure 7 but membrane plus bending stress is increased to about 250 MPa in high stress region around the corner bolts. The CuCrZr yield strength is ~280 MPa. The maximum deflection is ~5 mm. The linearized stresses on secondary plates are expected to be smaller due to smaller peak disruption forces and moments as indicated in Figure 5.

An ANSYS electromagnetic simulation was performed which eliminated the vector potential transfer and refined the mesh to capture the skin effects. A comparison of these results is included in figures 6 and 9.

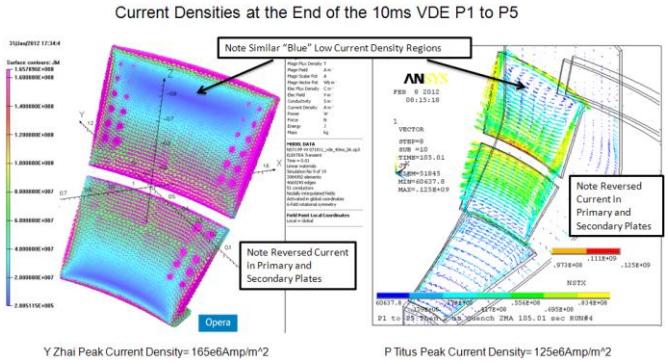

Figure 6 Comparison of eddy current density flowing in opposite direction in the two analyses due to reversed plasma current in two models.

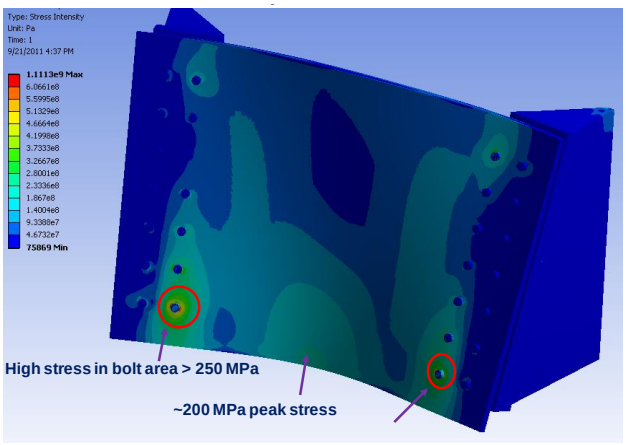

Figure 7 Stress distribution on lower primary plate at 10 ms during P1-P5 plasma translation.

VIII. Dynamic Implication

To understand the dynamic effect on passive plates during plasma disruption, structural dynamic analysis to obtain the dynamic amplification factor (DLF) has been performed. Basically, the time dependent elemental forces from Opera EM analysis are mapped onto ANSYS structural model; the deflection and stress level are compared to results from the static analysis. A damping ratio of 0.5% (mass to stiffness damping constant) is used. Figure 8 presents the deflection of lower primary plate at 10 ms during P1-P5 VDE translation. The results indicate a dynamic amplification factor of ~1.1. Dynamic rebound is the source of the tensile load that challenges the retaining bolts. Figure 9 indicates a reasonable agreement of stress level in the primary plate between results from Opera-Workbench analysis and that from the classic ANSYS.

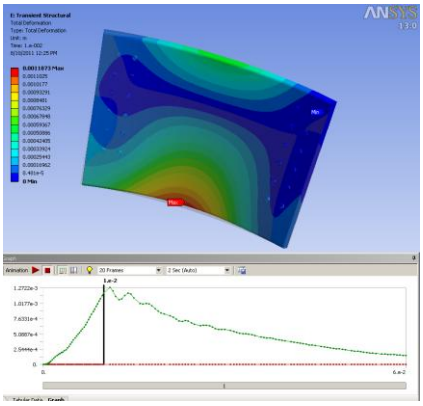

Figure 8 Lower primary passive plate during P1-P5 translation with a dynamic amplification factor of 1.1

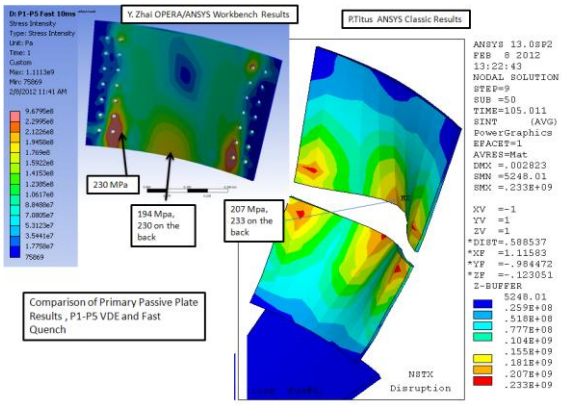

Figure 9 Comparison of primary passive plate stress intensity from Opera-Workbench and classic ANSYS.

IX. Halo Current

Halo currents are expected to have a less significant impact on the passive plates during disruption. Early analysis [5-6] suggested that the time constant for establishing Halo current flow is fairly long relative to the disruption timescale. Therefore, Halo current will enter the vacuum vessel through the bracket behind the passive plate. Halo current studies based on operational measurements show consistent radially outward loading, which loads the bracket in compression and does not load the bolts which provide the tensile restraint of the plates.

X. Bolt Analysis

The large pulling and pushing forces plus bending of the plate due to non-uniform distribution of eddy current flowing in the plate is a major concern for the existing 3/8" SS bolts, particularly for the corner bolts. The linearized stress in worst corner bolt at the end of fast quench (pulling force) is ~200 MPa membrane stress and the linearized stress in worst corner bolt at end of P1-P5 translation (pushing force) is ~328 MPa membrane stress. The tensile force on the worst corner bolt during disruption due to pulling of the plate is ~6,831 lbs. The pushing force on the worst corner bolt due to pushing of the plate is ~11,263 lbs. The normal stress on the bolt hat will be 468 MPa. Inconel 718 bolts of the same size will be used to replace the existing stainless steel bolts.

With the old washer design, Tresca shear stress in passive plate counter-bore due to pulling force is ~133 MPa. If we consider dynamic rebound force at the end of P1-P5 translation (rebound of pushing force – assume 80%) [5], the shear stress in passive plate counter bore is ~87 MPa and the equivalent Tresca stress is 174 MPa, or 25.2 ksi. With the new washer and bushing design, the effective shear area is increased to 2 square inches and the shear stress in counter bore due to pulling force is ~3.5 ksi and the equivalent Tresca stress is ~7 ksi. The shear stress due to dynamic rebound of pushing force is ~5.7 ksi and the equivalent Tresca stress is 11.33 ksi, smaller than the 24 ksi shear stress allowable for passive plates.

XI. CONCLUSIONS

The 3D disruption analysis indicated that stress in current half inch passive plates meets the design limits for the upgrade performance. The large disruption forces on the worst corner bolt, however, showed that corner bolts should be replaced with half inch bolt, or the same size Inconel 718 bolts.

*This work is supported by US DOE Contract No. DE-AC02-09CH11466. The authors thank Ali Zolfaghari for helping with skin depth evaluation; Neway Atnafu for support on hardware drawings of the new bushing design.

REFERENCES

1. J. E. Menard et al, "Overview of the physics and engineering design of NSTX upgrade", Nuclear Fusion, **52** 083015, 2012.
2. C. Neumeyer, "NSTX Upgrade General Requirements Document", NSTX_CSU-RQMTS-GRD Revision 3, December, 2010.
3. P. H. Titus et al, "NSTX disruption simulations of detailed divertor and passive plate models by vector potential transfer from OPERA global analysis results", **86** 1784-1790, 2011.
4. Y. Zhai, "Turbo pump magnetic shielding analysis for NSTX upgrade", NSTX-CALC-24-04-00, March, 2011.
5. P. H. Titus et al, "Disruption analysis of passive plates, vacuum vessel and components", NSTXU-CALC-12-01-01, February, 2012.
6. A. Brooks, "NSTX Halo current analysis of center stack", NSTX-CALC-133-05-00, April, 2010.

The Princeton Plasma Physics Laboratory is operated
by Princeton University under contract
with the U.S. Department of Energy.

Information Services
Princeton Plasma Physics Laboratory
P.O. Box 451
Princeton, NJ 08543

Phone: 609-243-2245
Fax: 609-243-2751
e-mail: pppl_info@pppl.gov
Internet Address: http://www.pppl.gov